Journal of Inorganic Biochemistry 197 (2019) 110705

Contents lists available at ScienceDirect

Journal of Inorganic Biochemistry

journal homepage: www.elsevier.com/locate/jinorgbio

Binding propterties of two Ru(II) polypyridyl complexes containing dppz units and fluorine groups with poly(U)·poly(A) ∗ poly(U) triplex

Fangfang Wang[a], Shuai Ma[a], Yongdeng Feng[a], Xiaohua Liu[b], Lifeng Tan[c,d,*]

[a] College of Chemistry, Xiangtan University, Xiangtan 411105, People's Republic of China
[b] School of Chemical Engineering, Xiangtan University, Xiangtan 411105, People's Republic of China
[c] Key Lab of Environment-friendly Chemistry and Application in Ministry of Education, Xiangtan University, Xiangtan 411105, People's Republic of China
[d] Key Laboratory for Green Organic Synthesis and Application of Hunan Province, Xiangtan University, Xiangtan 411105, People's Republic of China

ARTICLE INFO

Keywords:
Ru(II) complex
RNA triplex
Third-strand
Binding property
Stabilization

ABSTRACT

In this work, two Ru(II)-dppz (dppz = dipyrido[3,2-*a*:2′,3′-*c*]phenazine) complexes containing fluorine substituents, $[Ru(bpy)_2(7\text{-F-dppz})]^{2+}$ (Ru**1**, bpy = 2,2′-bipyridine, 7-F-dppz = 7-fluorodipyrido[3,2-*a*:2′,3′-*c*]phenazine) and $[Ru(phen)_2(7\text{-F-dppz})]^{2+}$ (Ru**2**, phen = 1,10-phenanthroline), have been synthesized and characterized. Binding properties of Ru**1** and Ru**2** with the RNA poly(U)·poly(A) ∗ poly(U) triplex have been studied by spectroscopic methods and viscosity measurements. The obtained results indicate that the binding differences of the two complexes with the triplex may be attributed to the ancillary ligand effects, implying that the better planarity and greater hydrophobicity of ancillary ligands are advantageous to the π–π stacking interaction between Ru**2** and the triplex, thus Ru**2** stabilizes the triplex strongly than Ru**1**. Denaturation of the triplex shows that both Ru**1** and Ru**2** can not only highly stabilize the template duplex of the triplex, but also significantly stabilize the third strand. Compared with the triplex stabilizing effects for the reported Ru(II)-dppz complexes, thermal melting experiments suggest that the fluorine substituent on the ligand dppz can probably decrease electrostatic repulsion between the three strands of the triplex, thereby Ru**1** and Ru**2** significantly increase the triplex stabilization. Results obtained from this work further confirm that the substituent electron effect of dppz-based ligands and the planarity and hydrophobicity of ancillary ligands play an important role in the triplex stabilizing effects by Ru(II)-dppz complexes.

1. Introduction

RNA triple-helical structures (also called RNA triplexes) are originally discovered by Rich and coworkers as early as in 1957 [1]. Evidence shows that RNA triplexes present a variety of potential applications in molecular biology, diagnostics and therapeutics [2]. More recently, the potential *in vivo* functions of RNA triplexes have been reviewed in detail by several teams [3], which opens up new vistas in understanding genome biology and gene regulation. Previous studies suggest that the stabilization of RNA triplexes has a crucial effect on their functions in many biological processes [4]. Due to the Hoogsteen base pairing, however, RNA triplexes are thermodynamically less stable than the corresponding Watson-Crick base paired duplex strand. For example, within the RNA triplex poly(U)·poly(A) ∗ poly(U) (where · denotes the Watson-Crick base pairing and * denotes the Hoogsteen base pairing), the Hoogsteen paired poly(U) strand (third-strand) separation from the triple-helical structure occurs at about 36 °C, while separation of the Watson-Crick base paired poly(U)·poly(A) duplex strand occurs around 47 °C [5]. The poor stability of RNA triplexes limits their practical use under physiological conditions [3a,3b,6]. Thus, how to achieve the third-strand stability is a very important topic. In this regard, small molecules able to recognize, bind and stabilize specific sequences of triplex RNA are in great demands [7].

Much effort in recent years has been directed to the design of small molecules with diverse structure traits to improve the triplex stabilization [8–17]. Previous studies demonstrate that small molecules as intercalators can either stabilize [18] or destabilize [19] a triplex RNA, suggesting the structural features of small molecules affecting the triplex stabilization are very complicated. Currently, the study is mainly focusing on organic compounds [17,20], there is little information on the triplex stabilizing effects by metal complexes [7,18a]. Our laboratory recently have studied the binding of a few Ru(II) polypyridyl

* Corresponding author at: Key Lab of Environment-friendly Chemistry and Application in Ministry of Education, Xiangtan University, Xiangtan 411105, People's Republic of China.
E-mail address: lfwyxh@yeah.net (L. Tan).

https://doi.org/10.1016/j.jinorgbio.2019.110705
Received 7 March 2019; Received in revised form 26 April 2019; Accepted 1 May 2019
Available online 02 May 2019
0162-0134/

complexes containing dppz units [18b,21] toward the poly(U)·poly(A) ∗ poly(U) triplex and found that subtle modifications of either the intercalative ligand dppz or the ancillary ligands surrounding the metal centre may significantly affect the third-strand stabilization. For example, the intercalating Ru(II)-dppz complexes, such as [Ru(phen)$_2$(mdpz)]$^{2+}$ (phen = 1,10-phenanthroline, mdpz = 7,7′-methylenedioxyphenyldipyrido- [3,2-*a*:2′,3′-*c*]-phenazine) [18b], [Ru(L)$_2$(7-CH$_3$-dppz)]$^{2+}$ {L = 2,2′-bipyridine (bpy) or 1,10-phenanthroline (phen), 7-CH$_3$-dppz = 7-methyldipyrido[3,2-*a*:2′,3′-*c*]phenazine} [21a] and [Ru(bpy)$_2$(dppz)]$^{2+}$ (dppz = dipyrido[3,2-*a*:2′,3′-*c*]phenazine) [21b], prefer to bind with the Watson–Crick base pairing duplex strand of the triplex rather than the third strand under the same conditions, thereby modestly stabilizing the third strand (ΔT_{m1} = 3.5–7.9 °C, ΔT_{m1} is the difference between the melting temperature of transition of the triplex to a duplex plus a single strand in the presence and absence of a binding reagent). In contrast, complex [Ru(phen)$_2$(dppz-idzo)]$^{2+}$ (dppz-idzo = dppz-imidazolone) greatly exert a thermally stabilizing effect on the third strand instead of the Watson–Crick base pairing duplex strand of the triplex [21c]. Even so, this complex can only increase the third-strand stabilization from 36.5 to 48.0 °C (ΔT_{m1} = 11.5 °C). As an effort to improve the third-strand stabilization of a triplex RNA by small molecules, study on the binding of RNA triplexes with Ru(II) polypyridyl complexes with different shapes and electronic properties are very necessary.

Given that complex [Ru(phen)$_2$(7-CH$_3$-dppz)]$^{2+}$ [21a] significantly stabilizes the template duplex (ΔT_{m2} = 13.4 °C, ΔT_{m2} is the difference between the melting temperature of dissociation of the template duplex into its components in the presence and absence of a binding reagent), while [Ru(bpy)$_2$(7-CH$_3$-dppz)]$^{2+}$ displays no obvious differences in stabilizing the template duplex (ΔT_{m2} = 6.5 °C) and the third strand (ΔT_{m1} = 4.0 °C) [21a], if the electron-donating methyl group in the two complex is substituted by the electron-attracting fluorine group and the ancillary ligands are still kept the same, what will happen to the triplex stabilizing effects by the new Ru(II)-dppz complexes? Thus, we set out to evaluate the substituent electron effect of dppz-based ligands affecting the binding of Ru(II)-dppz complexes with RNA triplexes.

In this work, two Ru(II)-dppz complexes containing fluorine substituents (Scheme 1), [Ru(bpy)$_2$(7-F-dppz)]$^{2+}$ (Ru**1**, 7-F-dppz = 7-fluorodipyrido [3,2-*a*:2′,3′-*c*]phenazine) and [Ru(phen)$_2$(7-F-dppz)]$^{2+}$ (Ru**2**), have been synthesized and characterized. The binding properties of Ru**1** and Ru**2** with the RNA poly(U)·poly(A) ∗ poly(U) triplex have been examined by various biophysical techniques. Compared with what determined for those reported Ru(II) complexes containing dppz units [18b,21], the obtained results of this study suggest that fluorine substituents on the main ligands play an important role in the two complexes stabilizing the triplex.

2. Experimental section

2.1. Materials

Compounds 1,10-phenanthroline-5,6-dione [22], *cis*-[Ru(bpy)$_2$Cl$_2$]·2H$_2$O and *cis*-[Ru(phen)$_2$Cl$_2$]·2H$_2$O [23] were synthesized according to literature procedures. Double stranded poly(A)·poly(U) (A = adenine) and single stranded poly(U) (U = uracil) were obtained from Sigma-Aldrich Corporation (St. Louis, MO, USA) and were used as received. Formation of the poly(U)·poly(A) ∗ poly(U) triplex was prepared as reported earlier [18b]. Concentrations of poly(A)·poly(U), poly(U) and poly(U)·poly(A) ∗ poly(U) were determined optically using molar extinction coefficients, ε ($M^{-1}\,cm^{-1}$) reported in the literature [2c]. Titration experiments were conducted at 20 °C in pH 7.0 phosphate buffer (6 mmol/L Na_2HPO_4, 2 mmol/L NaH_2PO_4, 1 mmol/L Na_2EDTA, 19 mmol/L NaC1). All reagents and solvents were purchased commercially and used without further purification unless specially noted and ultrapure water was used in all experiments.

2.2. Physical measurement

Microanalyses (C, H and N) were carried out on a Perkin-Elmer 240Q elemental analyzer. ^{1}H NMR (NMR = nuclear magnetic resonance) spectra were collected on an Avance-400 spectrometer with DMSO-d_6 (DMSO = dimethylsulfoxide) as solvent at room temperature and TMS (TMS = tetramethylsilane) as the internal standard. Mass spectrometry was performed on an Autoflex III™ Maldi-TOF-MS (Maldi-TOF-MS = matrix assisted laser desorption ionization time-of-flight mass spectrometry) (Bruker) using CH_3CN as the mobile phase. UV–visible (UV–vis) spectra were recorded on an Agilent spectrum Cary 100 spectrophotometer, and emission spectra were recorded on PTI Qm400 luminescence spectrometer at room temperature. Optical rotations were measured using a Perkin-Elmer (Boston, MA) 341 LC polarimeter equipped with mercury lamp. Circular dichroic (CD) spectra were measured on a JASCO-810 spectropolarimeter.

2.3. Synthesis of ligand 7-F-dppz·H_2O

A mixture of 1,10-phenanthroline-5,6-dione (210 mg, 1.0 mmol), 4-fluoro-*o*-phenylenediamine (126 mg, 1.0 mmol) and ethanol (20 mL) was refluxed for 4 h at 80 °C. The cooled solution was filtered and diluted with water. The yellow precipitate was filtered and washed with amounts of cold ethanol, then dried in vacuum. Yield: 240 mg, 80%. MALDI-TOF-MS (*m/z*): 301.3 ([M + 1]). Anal. calc. For $C_{18}H_{11}ON_4F$:C 67.92, H 3.48, N 17.60; found: C 67.89, H 3.52, N 17.57.

2.4. Synthesis of [Ru(bpy)$_2$(7-F-dppz)](ClO$_4$)$_2$·2H$_2$O (Ru**1**)

Complex Ru**1** was synthesized in the same way as [Ru(bpy)$_2$(dppz)]$^{2+}$ [23]. A mixture of *cis*-[Ru(bpy)$_2$Cl$_2$]·2H$_2$O (100 mg, 0.2 mmol) and 7-F-dppz (60 mg, 0.2 mmol) in ethylene glycol (20 mL) was refluxed under argon for 8 h at 150 °C to give a clear red solution. After it being cooled to room temperature, the solution was diluted with 15 mL water, and treated with addition of saturated aqueous $NaClO_4$ solution to afford a lot of red solid precipitate formed. The red product was collected by suction filtration and purified by column chromatography on alumina using acetonitrile-toluene (3:1, *v*/v) as eluent. The

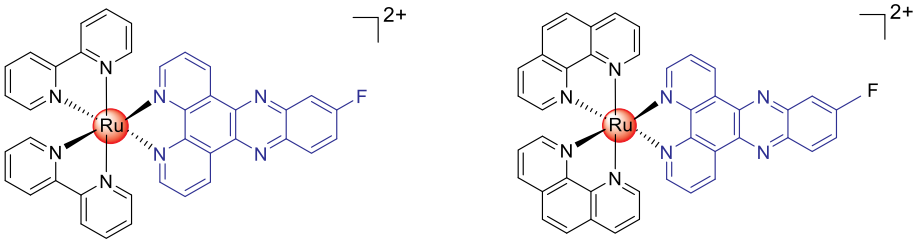

[Ru(bpy)$_2$(7-F-dppz)]$^{2+}$ [Ru(phen)$_2$(7-F-dppz)]$^{2+}$

Scheme 1. Chemical structures of [Ru(bpy)$_2$(7-F-dppz)]$^{2+}$ (Ru**1**) and [Ru(phen)$_2$(7-F-dppz)]$^{2+}$ (Ru**2**) (two counter ions perchlorates are omitted).

main red band was collected, solvent was removed by rotary evaporation, and red powder was further recrystallized with acetonitrile-ether. Yield: 114 mg, 80%. Anal. Calc. For $C_{38}H_{29}N_8O_{10}Cl_2FRu$: C 48.11, H 3.08, N 11.81; found: C 48.02, H 3.15, N 11.75. Maldi-TOF-MS (*m/z*): 714.1 ($[M\text{-}2ClO_4]^{2+}$). UV–Vis λ_{max}/nm ($\varepsilon/M^{-1}\,cm^{-1}$, CH_3CN): 281 (137175), 360 (25255), 448 (24860). ^1H NMR (400 MHz, ppm, d_6-DMSO): δ 9.62 (dd, J_1 = 1.2 Hz, J_2 = 2.4 Hz, J_3 = 1.2 Hz, 1H), 9.60 (dd, J_1 = 0.8 Hz, J_2 = 2.8 Hz, J_3 = 0.8 Hz, 1H), 8.88 (dd, J_1 = 8.4 Hz, J_2 = 3.6 Hz, J_3 = 8.4 Hz, 4H), 8.62 (dd, J_1 = 6.0 Hz, J_2 = 3.6 Hz, J_3 = 5.6 Hz, 1H), 8.32 (dd, J_1 = 2.8 Hz, J_2 = 6.4 Hz, J_3 = 2.8 Hz 1H), 8.29–8.18 (m, 4H), 8.18–8.11 (m, 3H), 8.07–8.00 (m, 2H), 7.83 (d, J = 5.6 Hz, 2H), 7.77 (d, J = 5.6 Hz, 2H), 7.61 (t, J_1 = 6.8 Hz, J_2 = 6.4 Hz, 2H), 7.39 (t, J_1 = 6.8 Hz, J_2 = 6.4 Hz, 2H).

2.5. Synthesis of [Ru(phen)$_2$(7-F-dppz)](ClO$_4$)$_2$·2H$_2$O (Ru**2**)

Complex Ru**2** was obtained by a procedure similar to that described for Ru**1**, with a mixture of *cis*-$[Ru(phen)_2Cl_2]\cdot 2H_2O$ (100 mg, 0.2 mmol) and 7-F-dppz (60 mg, 0.2 mmol). Yield: 106 mg, 70%. Anal. Calc. For $C_{42}H_{29}N_8O_{10}Cl_2FRu$: C 50.61, H 2.93, N 11.24; found: C 50.57, H 2.97, N 11.20. Maldi-TOF-MS (*m/z*): 762.0 ($[M\text{-}2ClO_4]^{2+}$). UV–Vis λ_{max}/nm ($\varepsilon/M^{-1}\,cm^{-1}$, CH_3CN): 265 (113435), 372 (18645), 443 (18375). ^1H NMR (400 MHz, ppm, d_6-DMSO): δ 9.59 (dd, J_1 = 0.8 Hz, J_2 = 2.4 Hz, J_3 = 0.8 Hz, 1H), 9.57 (dd, J_1 = 1.2 Hz, J_2 = 2.0 Hz, J_3 = 1.2 Hz, 4H), 8.79 (t, J_1 = 8.0 Hz, J_2 = 8.4 Hz, 4H), 8.20 (dd, J_1 = 6.0 Hz, J_2 = 3.6 Hz, J_3 = 6.0 Hz, 1H), 8.41 (s, 1H), 8.32 (dd, J_1 = 4.8 Hz, J_2 = 6.4 Hz, J_3 = 2.8 Hz, 1H), 8.28 (d, J = 4.8 Hz, 2H), 8.24–8.18 (m, 1H),8.16 (d, J = 2.8 Hz, 1H), 8.14 (d, J = 2.8 Hz, 1H), 8.06 (d, J = 4.4 Hz, 2H), 7.96–7.87 (m, 2H), 7.86–7.74 (m, 4H).

2.6. Absorption spectral experiment

UV–vis spectra titration was determined on an Agilent spectrum Cary 100 spectrophotometer at 20 °C. Firstly, adding 3000 μL solutions of phosphate buffer and ruthenium complex sample (9.2 μM) to the reference and sample cuvettes, respectively. Recording the curves of complex between 230 nm and 750 nm. Then the RNA triplex stock solution was added to each curve up to saturation. After each addition, the system should mix for about 5 min to allow the system to equilibrate before recording the absorption spectra. The intrinsic binding constant K_b and the binding site *s* of metal complex toward the triplex from absorbance titration were calculated by a nonlinear least squares method using the following equation (1) [20b]:

$$\frac{\varepsilon_a - \varepsilon_f}{\varepsilon_b - \varepsilon_f} = \frac{\sqrt{b - (b^2 - 2K_b^2 C_t [RNA]/s)}}{2K_b C_t} \quad (1a)$$

$$b = \frac{1 + K_b C_t + K_b [RNA]}{2s} \quad (1b)$$

where [RNA] is the total concentration of poly(U)·poly(A) ∗ poly(U) in the nucleotide phosphate; *s* is the binding site size in base pairs of Ru(II) complexes interacting with the triplex; ε_a, ε_f and ε_b are the apparent, free and bound metal complex extinction coefficients, respectively; K_b represents the microscopic binding constant for each site in M^{-1}; C_t is the total concentration of R(II) complexes.

2.7. Emission spectra experiment

Luminescence titration was acquired on a PTI Qm400 luminescence spectrometer at 20 °C. Setting the excited wavelength at 468 nm, and the emission spectrum was collected from 500 nm- 800 nm. Similar to the absorption spectral, placing 3.0 mL solutions of phosphate buffer and ruthenium complex sample (2.0 μM) to a quartz cuvette, the first curve was recorded. After each addition of the RNA triplex, the solution was mixed and allowed to re-equilibrate for at least 3 min before recording the curve. This titration process was repeated until there was no change in the spectra.

The intrinsic binding constant K_b the two Ru(II) complexes toward the triplex from Luminescence titrations was calculated by a nonlinear least squares method using the following equation (2) [24]:

$$(I - I_0)/(I_f - I_0) = (b - (b^2 - 2K^2 C_t [RNA]/s)^{1/2})/(2KC_t) \quad (2a)$$

$$b = 1 + KC_t + K[RNA]/(2s) \quad (2b)$$

where *I*, I_0 and I_f are the emission intensity in the presence of RNA, in the absence of RNA, and the final maximum emission intensity for the Ru(II) complex in the fully bound form, respectively. *K* is the equilibrium binding constant in M^{-1}, C_t is the total metal complex concentration, [RNA] is the total concentration of poly(U)·poly(A) ∗ poly (U) in the nucleotide phosphate, and *s* is the binding site size.

2.8. Thermal melting experiment

Thermal melting of the RNA triplex in the absence and presence of Ru**1** or Ru**2** was carried out with an Agilent spectrum Cary 100 spectrophotometer equipped with a Cary 100 temperature-control programmer (± 0.1 °C). The temperature of the solution was raised from 25 to 65 °C at a rate of 1.0 °C min^{-1} by monitoring the absorbance change at about 260 nm for the solutions of the triplex (32.1 μM) in the presence of different concentrations of the complex. The date were presented as $(A - A_0)/(A_f - A_0)$ (A = absorption) *versus* temperature, where A, A_0, and A_f are the observed, the initial, and the final absorbance at 260 nm, respectively. The titration procedure was similar to the absorption spectral.

2.9. Viscosity study

The viscometric measurement was carried out with an Ubbelohde viscometer maintained at a constant temperature of (20 ± 0.1) °C in a thermostatic bath. Adding the sample solutions (10 mL) to the viscometer, then measure the flow time using a digital stopwatch, and each sample was measured three times. Relative viscosities for the triplex RNA in either the absence or presence of metal complex was calculated according to literature procedures reported earlier [25].

2.10. CD spectral experiment

CD spectrum was acquired on a Jasco-810 spectropolarimeter at 20 °C by incrementally adding the metal complex into the solutions containing RNA triplex. After each addition, the solution was mixed evenly and allowed to re-equilibrate for at least 5 min before recording the CD spectra. Each spectrum was averaged from three successive accumulations and was baseline corrected, smoothed, and normalized to nucleotide phosphate concentration in the region 200–600 nm using the software supplied by Jasco [26].

3. Results and discussion

3.1. Synthesis and characterization

The synthetic routes to the main ligand 7-F-dppz and its Ru(II) complexes are presented in Scheme 2. The main ligand 7-F-dppz is prepared by condensation of 1,10-phenanthroline- 5,6-dione and 4-fluoro-*o*-phenylenediamine using a method similar to that described by Dickeson and Summers [27]. The corresponding Ru**1** and Ru**2** are synthesized by direct reaction of *cis*-$[Ru(bpy)_2Cl_2]\cdot 2H_2O$ or *cis*-$[Ru(phen)_2Cl_2]\cdot 2H_2O$ with the ligand 7-F-dppz. Perchlorate salts are used here as a precipitant to facilitate the required complexes to be separated from the solution. If Perchlorate salts are not used, the solvent needs to be removed to obtain the complex, since complexes with chlorine anions are soluble in ethylene glycol. Therefore, the desired complexes are isolated as their perchlorate salts in 80% and 70% yield, respectively.

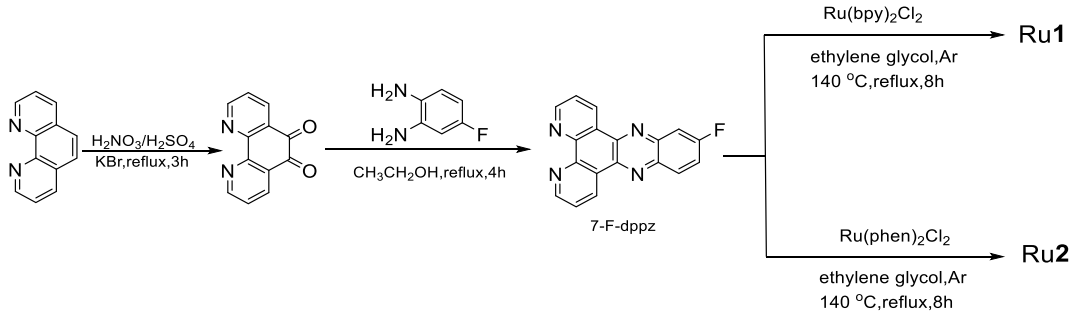

Scheme 2. Synthetic routes to the ligand 7-F-dppz and its complexes Ru**1** and Ru**2**.

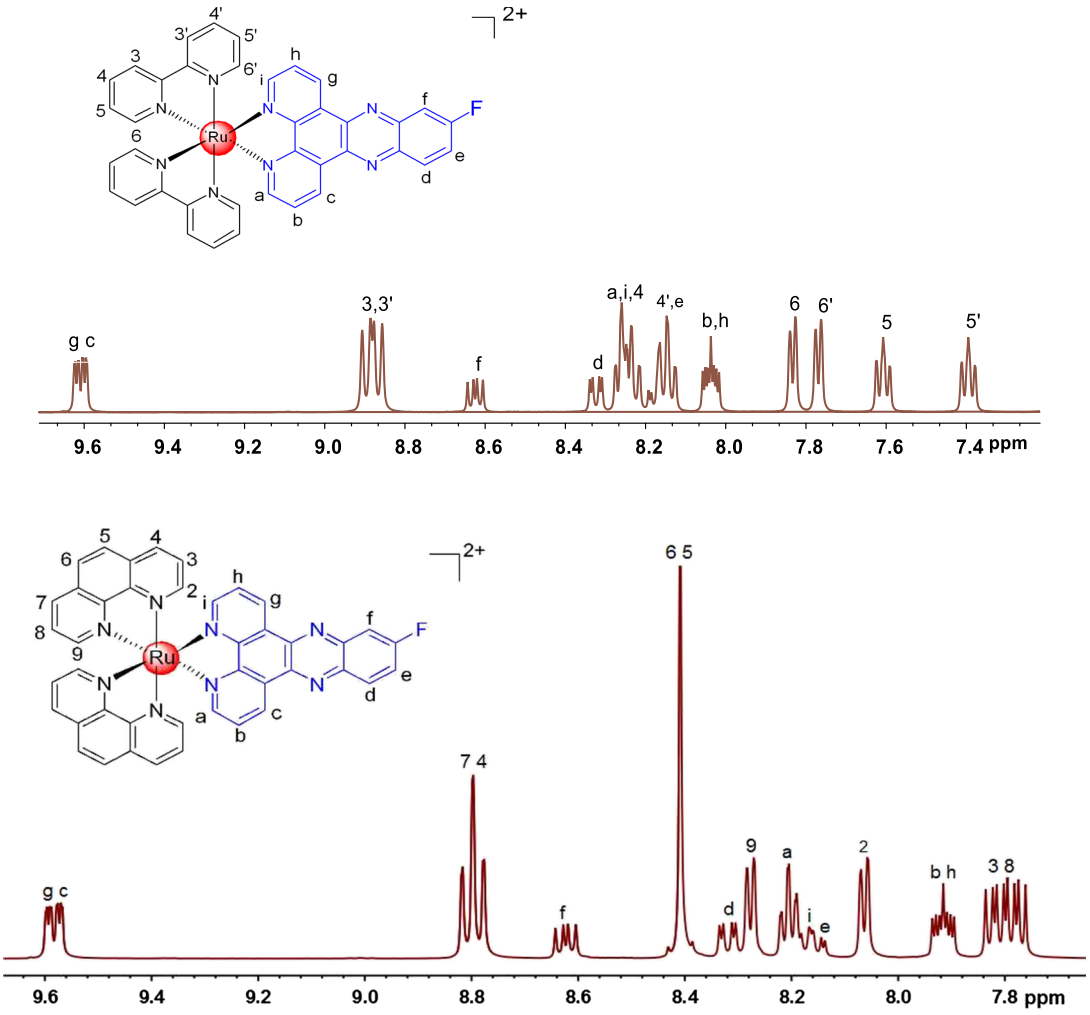

Fig. 1. ^{1}H NMR (400 MH$_Z$) spectrum of Ru**1** and Ru**2** in d_6-DMSO (two counter ions perchlorates are omitted for the chemical structures of Ru**1** and Ru**2**).

Both complexes are characterized by mass spectrometry and NMR spectroscopy (Fig. 1). In the Maldi-TOF-MS of either Ru**1** or Ru**2**, only one signal of $[M\text{-}2ClO_4^-]^{2+}$ is observed and the determined molecular weight is consistent with the expected value. Both Ru**1** and Ru**2** give well-defined ^{1}H NMR spectra, which permitted unambiguous identification and assessment of purity.

The UV–Vis absorption spectra of Ru**1** and Ru**2** are characterized by intense ligand-centred transitions in the UV region and metal-to-ligand charge transfer (MLCT) transition in the visible region. The peaks at 281 nm for Ru**1** and 265 nm for Ru**2** are attributed to intraligand $\pi \rightarrow \pi^*$ transitions. The low energy bands at 448 for Ru**1** and 443 nm for Ru**2** are assigned as Ru(dπ) → 7-F-dppz(π^*) transitions [28]. Besides, the bands at 360 nm for Ru**1** and 372 nm for Ru**2** can be assigned to the intraligand (IL) transition of 7-F-dppz. Similar to $[Ru(phen)_2(dppz)]^{2+}$ [29] and $[Ru(bpy)_2(dppz)]^{2+}$ [30] and their derivatives containing dppz unit [18b,21], both complexes exhibit no luminescence aqueous solutions at room temperature, but display intense luminescence in acetonitrile with the maximum at 628 nm for Ru**1** and 623 nm for Ru**2** respectively.

3.2. Electronic absorption spectral

Electronic absorption spectroscopy is one of the most useful techniques in triplexes-binding studies [31]. In general, progressive addition of increasing concentrations of the triplex to the solution of an aromatic small molecule resulting in different levels of hypochromic

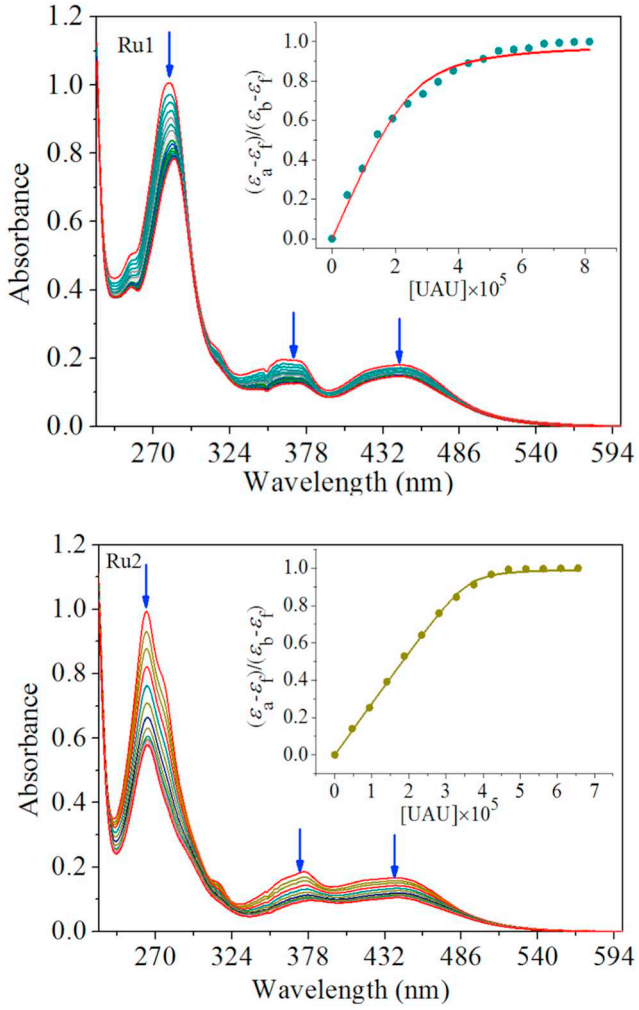

Fig. 2. Representative absorption spectral changes of Ru**1** and Ru**2** in the presence of RNA triplex in phosphate buffer (6 mmol/L Na_2HPO_4, 2 mmol/L NaH_2PO_4, 1 mmol/L Na_2EDTA, 19 mmol/L NaC1, pH 7.0) at 20 °C. [Ru**1**] = [Ru**2**] = 9.2 μM, For Ru**1** and Ru**2**, [UAU] = 0–79.8 and 0–65.3 μM, where UAU stands for poly(U)·poly(A) * poly(U). The arrows show the absorbance changes upon an increasing poly(U)·poly(A) * poly(U) concentration. Inset: plots of $(\varepsilon_a - \varepsilon_b)/(\varepsilon_f - \varepsilon_b)$ *vs.* [UAU] by nonlinear fit.

and bathochromic effects in the visible region absorbance spectra of a small molecule, due to the intermolecular interaction involving overlap of the π electron cloud of an aromatic ring with the base triplets [32]. The spectral changes for Ru**1** and Ru**2** in the presence of poly(U)·poly(A) * poly(U) triplex are depicted in Fig. 2. The relevant data are listed in Table 1.

As shown in Fig. 2, the magnitude and shape of the visible absorption bands of either Ru**1** or Ru**2** are noticeably altered upon progressive adding the triplex. The binding of Ru**1** to the triplex RNA results in *ca.* 36% and 18% reductions in the absorbance of the IL (IL = intraligand) and MLCT (MLCT = metal-to-ligand charge transfer) bands with 6- and 2-nm red shifts at 362 and 445 nm, respectively. For Ru**2**, however, the IL and MLCT bands display about 48% and 37% reductions with 3- and 5-nm red shifts at 375 and 439 nm respectively. The obvious changes in the absorption spectra spectral of Ru**1** and Ru**2** suggest that the two complexes bind to the triplex most likely through an intercalative mode, which involves a stacking interaction between the aromatic chromophore and the base pairs of the triplex. On the other hand, both polarity effects of the triplex and electron transfer from the base triplets may also contribute to the spectral changes of the two complexes to a certain extent.

Using changes at the MLCT band, the intrinsic binding constant K_b and binding site size *s* are determined to be $(5.16 \pm 1.28) \times 10^5\,M^{-1}$ and (1.29 ± 0.15) for Ru**1** and $(5.92 \pm 0.13) \times 10^6\,M^{-1}$ and (1.91 ± 0.12) for Ru**2** respectively, which is indicative of a stronger association of Ru**2** with the triplex. Since the intercalative ligands of Ru**1** and Ru**2** are the same, a greater binding affinity for Ru**2** may be attributed to the ancillary ligand effects. Ongoing from bpy to phen, the planarity and hydrophobicity increase. Therefore, the better planarity and greater hydrophobicity are advantageous to the π–π stacking interaction between Ru**2** and the triplex, which make Ru**2** insert the bases of the triplex more deeply than Ru**1**, resulting in a greater binding affinity for Ru**2**. Notably, the binding constant K_b of Ru**2** has the same order of magnitude as those of Ru(II) complexes containing dppz units [18b,21], such as $[Ru(phen)_2(mdpz)]^{2+}$ ($K_b = 3.60 \times 10^6\,M^{-1}$), $[Ru(bpy)_2(7\text{-}CH_3\text{-}dppz)]^{2+}$ ($K_b = 1.03 \times 10^6\,M^{-1}$), $[Ru(phen)_2(7\text{-}CH_3\text{-}dppz)]^{2+}$ ($K_b = 3.05 \times 10^6\,M^{-1}$) and Δ-$[Ru(bpy)_2(dppz)]^{2+}$ ($K_b = 1.18 \times 10^6\,M^{-1}$), while the binding constant K_b of Ru**1** is comparable to that of Λ-$[Ru(bpy)_2(dppz)]^{2+}$ ($K_b = 6.43 \times 10^5\,M^{-1}$). Regarding these reported Ru(II)-dppz complexes, all of which bind with the triplex through an intercalative mode. Thus, we speculate that both Ru**1** and Ru**2** should have the same binding modes as these reported Ru(II)-dppz complexes. Notably, if we only compare the binding constants of Ru**1** and Ru**2** with those of the reported Ru(II)-dppz complexes, it seems difficult to evaluate the effects of the fluorine substituents on the binding behaviors.

3.3. Fluorescent and colorimetric studies

Synthetic fluorescent probes capable of binding to RNA structures have been used as powerful tools for the study of RNA functions, while the rational design of a luminescent probe for the specific secondary structures is made difficult by the complexity of RNA structures [33]. To determine whether Ru**1** and Ru2 could be as luminescent probes for poly(U)·poly(A) * poly(U) triplex, luminescence measurements are performed at room temperature. The representative spectral profiles of Ru**1** and Ru**2** in the absence and presence of the triplex are shown in Fig. 3. As can be seen from Fig. 3, Ru**1** and Ru**2** in phosphate buffer

Table 1
Binding constants (K_b), hypochromicity(*H*), bathochromic shifts (Δλ) of Ru**1** and Ru**2**. [Na^+] = 35 mM.

Complexes	λ_{max}(free)	λ_{max}(bound)	Δλ(nm)[a]	*H*%[b]	$K_b(\times 10^5\,M^{-1})$[c]	s[d]
Ru**1**	282	285	3	22	–	–
	362	368	6	36	–	–
	443	445	2	18	5.16 ± 1.28	1.29 ± 0.15
Ru**2**	264	265	1	42	–	–
	375	378	3	48	–	–
	439	444	5	37	59.21 ± 14.25	1.91 ± 0.02

[a] Δλ represents the difference in λ_{max} (free) and λ_{max} (bound).
[b] $H\% = 100\% \times (A_{free} - A_{bound})/A_{free}$ (*A* represents the absorbance).
[c] K_b was determined by monitoring the changes of absorption at the MLCT and IL band.
[d] *s* is an average binding size.

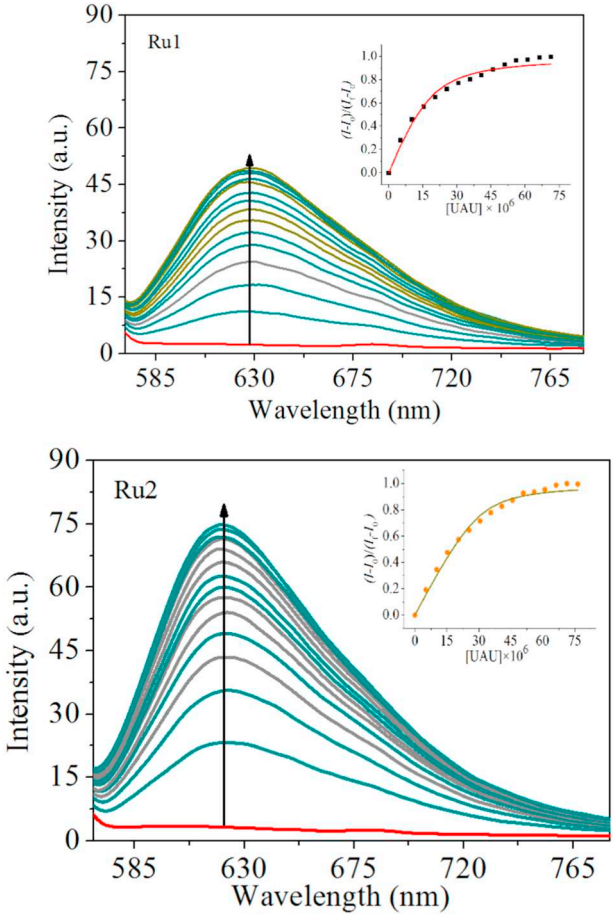

Fig. 3. Fluorescence spectra of Ru**1** and Ru**2** (λ_{ex} = 468 nm) treted with poly (U)·poly (A) ∗ poly(U). [Ru**1**] = [Ru**2**] = 2.0 μM, For Ru**1** and Ru**2**, [UAU] = 0–76.4 and 0–71.3 μM. The arrows show the intensity changes upon increasing the triplex concentration. Solution conditions are the same as those described in the legend of Fig. 2. Inset: plots of $(\varepsilon_a - \varepsilon_b)/(\varepsilon_f - \varepsilon_b)$ *vs.* [UAU] by nonlinear fit.

display negligible fluorescence in the absence of the triplex, and similar results are observed for those reported Ru(II) complexes containing dppz units, suggesting that their emissions are temporarily turned off [29,30]. However, the fluorescence of either Ru**1** or Ru**2** is turned on as soon as the triplex is added to the solution of each complex. Upon adding the triplex to saturated state, the luminescence of Ru**1** and Ru**2** rises sharply by around 21- and 25-fold enhancements in emission intensity respectively, behaving like RNA "molecular light switches". This reflects that the position of the bound Ru**1** and Ru**2** is in a hydrophobic environment similar to an intercalated condition and Ru**2** is protected more efficiently by the triplex than Ru**1**. Therefore, the accessibility of water molecules to Ru**2** in the presence of the triplex is more difficult compared with Ru**1** [34], resulting in Ru**2** displaying a greater emission increase upon binding to the triplex in saturation state. Using changes in the luminescence spectra, the K_b value is derived to be $(2.65 \pm 0.60) \times 10^5\,M^{-1}$ for Ru**1** and $(9.21 \pm 0.95) \times 10^5\,M^{-1}$ for Ru**2** respectively, which very closes to that from absorption titration and also reflects a stronger association of Ru**2** with the triplex. In addition, the emission enhancement of Ru**1** is comparable to those of $[Ru(bpy)_2(7\text{-}CH_3\text{-}dppz)]^{2+}$ (20-fold) [21a] and Λ-$[Ru(bpy)_2(dppz)]^{2+}$ (21-fold) [21b]. For Ru**2**, the changes in emission intensity closes to what observed for $[Ru(phen)_2(7\text{-}CH_3\text{-}dppz)]^{2+}$ (26-fold) [21a]. However, changes in the emission intensity of both Ru**1** and Ru**2** are much smaller than those of $[Ru(phen)_2(mdpz)]^{2+}$ (131-fold) [18b] and Δ-$[Ru(bpy)_2(dppz)]^{2+}$ (32-fold) [21b].

Interestingly, the enhancement of the intrinsic fluorescence of Ru**2** when bound to the triplex provides a possibility for the visual detection of the triplex. As shown in Fig. 4b (2), the dramatic "molecular light switch" effect can easily be observed by the naked eye under UV light without further treatment, while this phenomenon cannot be observed in the case of Ru**1** (Fig. 4a) or other reported Ru(II) complexes containing dppz units [18b,21], suggesting that Ru**2** is a prominent colorimetric "molecular light switch" for the triplex in a solution. Therefore, it seems that the substituents and/or ancillary ligands have a significant impact on colorimetric effects of Ru(II) complexes containing dppz units. Subsequently, pH affecting the colorimetric effect of Ru**2** is performed within the pH range from 2.3 to 7.2 by additions of HCl or NaOH solution (Fig. 4b). In the acidic pH region below 2.3, no color response can be observed by the naked eye under UV light (Fig. 6B, (3)), while the color response recurrences by adjusting pH from 2.3 to 7.2 (Fig. 4b, (4)), thus turning the colorimetric effect on and off over a series of cycles. To our knowledge, Ru**2** is the first small molecule whose colorimetric effects of the "off" and "on" states can be clearly distinguished by the naked eye upon adjusting the pH value.

3.4. Thermal denaturation

The triplex stabilizing effects by Ru**1** and Ru**2** are investigated by thermal melting experiments (Fig. 5), which also provide information on the binding specificity [35]. The quantitative data are listed in Table 2. As illustrated in Fig. 5, the RNA poly(U)·poly(A) ∗ poly(U) triplex in the absence of Ru(II) complexes exhibits a biphasic thermal dissociation profile. The first transition at lower temperature (35.9 °C, T_{m1}) belongs to dissociation of the triplex to a poly(U)·poly(A) duplex and a single-stranded poly(U) by dissociation of the Hoogsteen base-paired poly(U) strand from the major groove of the template duplex, and the second transition (45.0 °C, T_{m2}) corresponds to dissociation of the Watson-Crick base-paired duplex poly(U)·poly(A) into its components [20b]. The T_m value of the third strand increases to 46.9 and 50.8 °C and the second T_m increases to 58.9 and 60.8 °C upon adding, respectively, Ru**1** and Ru**2** at a [Ru]/[UAU] ratio of 0.35 (Ru stands for Ru**1** or Ru**2**, UAU stands for poly(U)·poly(A) ∗ poly(U)). Obviously, the stabilizing effect of Ru**2** is slightly marked in comparison with that of Ru**1**, which may be attributed to the ancillary ligands phen of Ru**2** possessing better planarity and greater hydrophobicity. From the data presented here, similar to what observed for the reported Ru(II)-dppz complex $[Ru(bpy)_2(7\text{-}CH_3\text{-}dppz)]^{2+}$, both Ru**1** and Ru**2** slightly prefer to bind with the Watson-Crick base-paired duplex rather than the Hoogsteen base-paired strand of the triplex under the conditions used in this study. In contrast, the triplex stabilizing effects of Ru**1** and Ru**2** differ from what observed for other Ru(II)-dppz complexes, $[Ru(phen)_2(mdpz)]^{2+}$ [18b] and $[Ru(phen)_2((7\text{-}CH_3\text{-}dppz))]^{2+}$ [21a]. Regarding $[Ru(phen)_2(mdpz)]^{2+}$ and $[Ru(phen)_2((7\text{-}CH_3\text{-}dppz))]^{2+}$, the two complexes prefer to stabilize the Watson-Crick base-paired duplex instead of the Hoogsteen base-paired strand of the triplex under the same conditions.

It is worth pointing out that the effects of Ru**1** and Ru**2** stabilizing the Hoogsteen base-paired strand of the triplex are more marked than those reported Ru(II)-dppz complexes containing dppz units, such as $[Ru(phen)_2(mdpz)]^{2+}$ [18b], $[Ru(L)_2((7\text{-}CH_3\text{-}dppz))]^{2+}$ (L = bpy and phen) [21a] and $[Ru(bpy)_2(dppz)]^{2+}$ [21c], reflecting that introducing an electron-withdraw fluorine substituent to the main ligand dppz of Ru(II) complexes may decrease interchain electrostatic repulsion, thereby significantly increasing the triplex stabilization. In addition, the effects of Ru**1** and Ru**2** sharply differ from those of $[Ru(L)_2(uip)]^{2+}$ {uip = 2-(5-uracil)-1*H*-imidazo[4,5-*f*][1,10]phenanthroline}[26], $[Ru(bpy)_2(pip)]^{2+}$ (pip = 2-phenyl-1*H*-imidazo[4,5-*f*]-[1,10]-phenanthroline) [35] and $[Ru(L)_2(btip)]^{2+}$ (L = bpy or phen, btip = 2-benzo[*b*]thien-2-yl-1*H*-imidazo [4,5-*f*][1,10]-phenanthroline) [36], all of which prefer to stabilize the third strand rather than the template duplex under the same condition. Furthermore, the triplex stabilizing effects by Ru**1** and Ru**2** are obviously

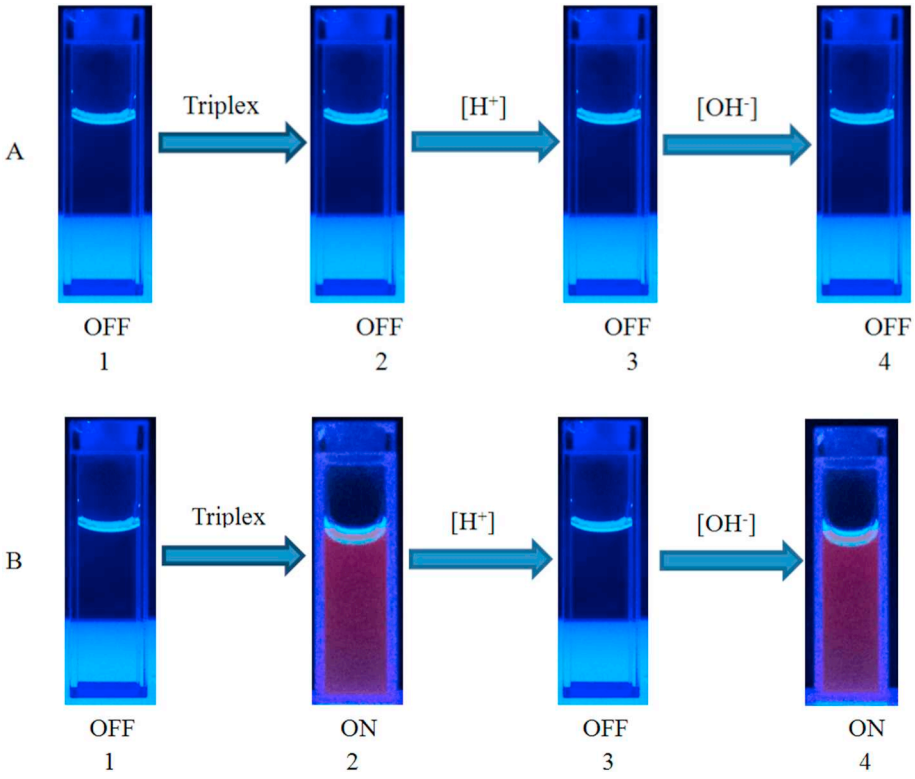

Fig. 4. Images of the "light switch" behaviors of Ru**1** (A, 60 μM) and Ru**2** (B, 60 μM) for poly(U)·poly (A) ∗ poly(U) (204 μM). (1) Ru**1** or Ru**2** complex, pH 7.2. (2) Ru**1** or Ru**2** complex and poly(U)·poly (A) ∗ poly(U), pH = 7.2. (3) Ru**1** or Ru**2** and poly (U)·poly (A) ∗ poly(U), pH adjusted to 2.3 by H^+. (4) Ru**1** or Ru**2** complex and poly(U)·poly(A) ∗ poly(U), pH adjusted back to 7.2 by OH^-.

different from $[Ru(phen)_2(dicnq)]^{2+}$ and $[Ru(bpy)_2(dicnq)]^{2+}$ (dicnq = 6,7-dicyanodipyrido- [2,2-*d*:2′,3′-*f*]quinoxaline) [37], the two Ru (II) complexes stabilize he Watson-Crick base-paired duplex of the triplex without affecting the third-strand stabilization. These reveal that the effects of small molecules on the triplex stabilization are very complicated and closely related to the size and shape as well as the substituent nature of small molecules.

3.5. Conformation changes of the triplex induced by complexes

CD spectroscopy is a conventional method for determining the conformation changes of RNA triplexes. Due to stacking interactions between the base triplets and the helical structure of the triplex strands, the intrinsic CD spectral pattern of the RNA poly(U)·poly(A) ∗ poly(U) triplex in the absence of either Ru**1** or Ru**2** is characterized by a large positive band at about 260 nm and an adjacent weak negative band at about 240 nm followed by a small positive band at about 220 nm [38]. In addition, the racemic complexes Ru**1** and Ru**2** display no intrinsic CD signals in the 200–600 nm region. Thus, any CD signal displaying above 300 nm belongs to the interaction of either Ru**1** or Ru**2** with the triplex and any appearance of the induced CD signals below 300 nm are attributed to the triplex or Ru(II) complex induced by each other [38]. In addition, the CD spectra of Ru(II) complex are subtracted from the spectra of the mixtures. As seen from Fig. 6, upon adding either Ru**1** or Ru**2**, the CD spectrum of the triplex are clearly perturbed and the perturbation is more remarkable in the case of Ru**2**. Binding of Ru**1** and Ru**2** results in the characteristic positive band at 260 nm displaying the same variation trends: upon addition of either Ru**1** or Ru**2** to saturated states, initial enhancements at low binding ratios and subsequent decreases in ellipticity at higher binding rations are observed with 2- and 4-nm blue shifts for Ru**1** and Ru**2**, respectively. However, the variation tendency in this characteristic band at 260 nm induced by either Ru**1** or Ru**2** is significantly different from what observed in the presence of other reported Ru(II)-dppz complexes containing dppz units [18b,21], such as $[Ru(phen)_2(mdpz)]^{2+}$, $[Ru(L)_2((7\text{-}CH_3\text{-}dppz))]^{2+}$ (L = bpy and phen) $[Ru(bpy)_2(dppz)]^{2+}$ and $[Ru(bpy)_2(dppz\text{-}idzo)]^{2+}$. Bind of all these reported Ru(II) complexes containing dppz units results in this band showing varying degrees of hyperchromic effects, which suggests that their binding geometries or binding sites may not be quite the same as those of Ru**1** and Ru**2**. On the other hand, the general shapes of the ICD (induced circular dichroism) above 290 nm are quite similar each other in the presence of Ru**1** and Ru**2**: a negative and positive bands occur at about 295 and 459 nm, respectively, but changes in the two ICD bands are more marked in the case of Ru**2**. A relatively stronger changes in the intrinsic and extrinsic CD bands of the triplex confirms a stronger binding of Ru**2** with the triplex. In addition, substantial perturbations of the CD spectrum of the triplex in the presence of Ru**1** and Ru**2** also imply that the binding mode of the two complexes with the triplex should be intercalation [39].

3.6. Viscosity measurements

Viscosity measurements is regarded as the most critical test of binding modes of small molecules with RNA triplexes in the absence of crystallographic structural data [34b,40]. To further clarify the binding modes of Ru**1** and Ru**2** toward the triplex, the changes in relative viscosities of poly(U)·poly(A) ∗ poly(U) triplex are measured by varying the concentrations of either Ru**1** or Ru**2** (Fig. 7). Fig. 7 indicates that the relative viscosity of the triplex solution increases steadily with increasing the concentrations of either Ru**1** or Ru**2**, and the viscometric variation trends are similar to what observed for other reported Ru(II) complexes containing dppz units [18b,21], suggesting that a true intercalation scenario may be envisaged for the two complexes binding toward the triplex [40]. In addition, the viscometric variation trends are found to be more rapidly pronounced upon adding Ru**2**, which further confirms that binding of Ru**2** with the triplex is stronger than that of Ru**1** under the same conductions. However, the viscometric variation trends of the triplex in the presence of Ru**1** and Ru**2** significantly differ from what observed for Ru(II) complex $[Ru(bpy)_2(btip)]^{2+}$ [36] and organic small molecule palmatine [41]. Regarding the intercalating complex, $[Ru(bpy)_2(btip)]^{2+}$, this complex results in initial decreases at low binding ratios and subsequent increases in the relative viscosity of

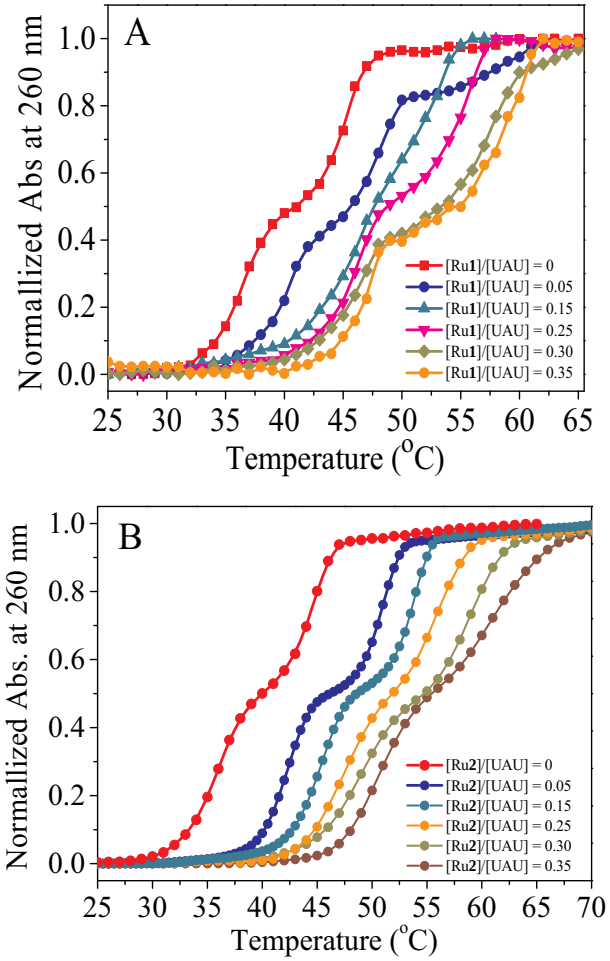

Fig. 5. Thermal denaturation curves at 257 nm of poly(U)·poly(A) * poly(U) (32.1 μM) and its complexation with Ru**1** (A) and Ru**2** (B) at different [Ru]/[UAU] ratios. Solution conditions are the same as those described in the legend of Fig. 2, and $[Na^+]$ = 35 mM.

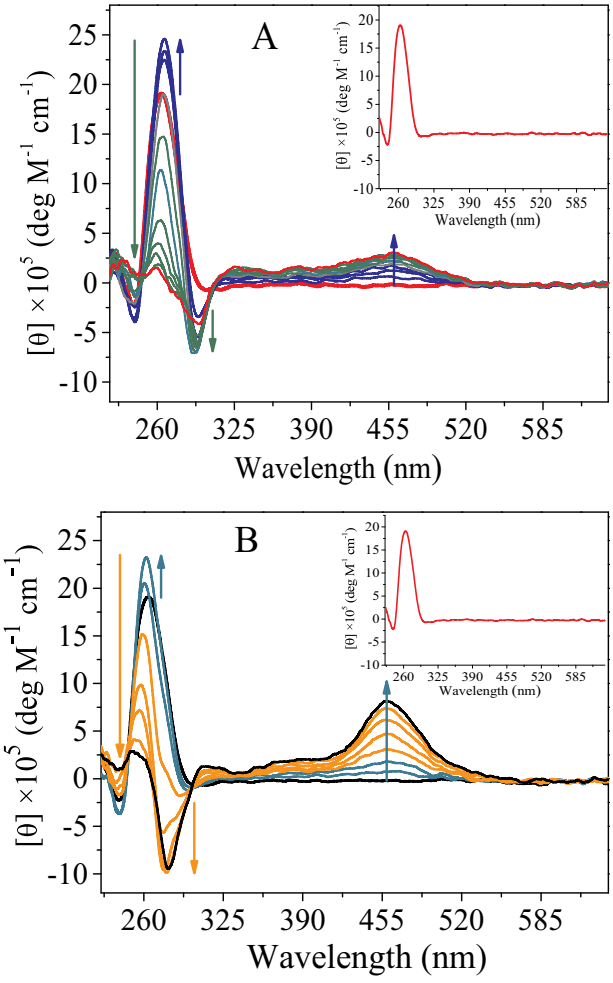

Fig. 6. CD spectra of poly(U)·poly(A) * poly(U) (100 μM) treated with Ru**1**(A) or Ru**2** (B) at different [Ru]/[UAU] ratios from 0 to 0.88 or 0–0.56. Solution conditions are the same as those described in the legend of Fig. 2.

Table 2
Melting temperatures (°C) for the investigated poly(U)·poly(A) * poly(U) in the absence and presence of Ru**1** and Ru**2**. UAU stands for the poly(U)·poly(A) * poly(U).

Title/complex	C_{Ru}/C_{UAU}	T_{m1} (°C)	T_{m2} (°C)	ΔT_{m1}	ΔT_{m2}
poly(U)·poly(A) * poly(U)	0	35.9	45.0	–	–
poly(U)·poly(A) * poly(U) + Ru**1**	0.05	39.9	46.9	4.0	1.9
	0.15	46.1	52.1	10.2	7.1
	0.25	46.1	54.9	10.2	9.9
	0.30	46.9	56.3	11.0	11.3
	0.35	46.9	58.9	11.0	13.9
poly(U)·poly(A) * poly(U) + Ru**2**	0.05	42.3	50.9	6.4	5.9
	0.15	45.5	53.9	9.6	8.9
	0.25	47.6	55.9	11.7	10.9
	0.30	48.9	58.9	13.0	13.9
	0.35	50.8	60.8	14.9	15.8

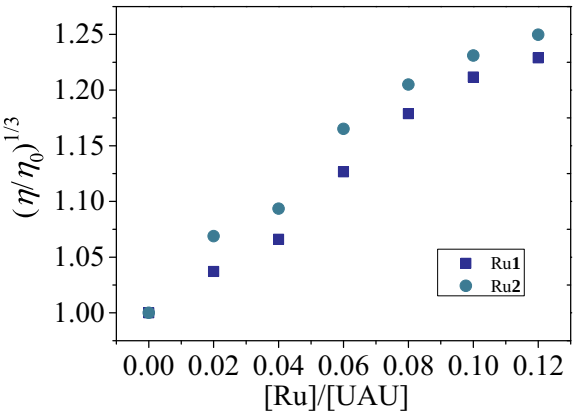

Fig. 7. Changes in relative viscosities of poly(U)·poly(A) * poly(U) in the present of Ru**1** and Ru**2** at 20 °C. [UAU] = 153 μM. Solution conditions are the same as those described in the legend of Fig. 2.

the triplex although the binding mode is intercalation. Concerning palmatine, this small molecule decreases the relative viscosity of the triplex because of it binding to the triplex through a partial intercalation. These indicate that the size and shape as well as the substituent nature of small molecules has a significant effect on the binding modes.

4. Conclusions

In summary, two Ru(II) complexes, $[Ru(bpy)_2(7\text{-F-dppz})]^{2+}$ (Ru**1**) and $[Ru(phen)_2(7\text{-F-dppz})]^{2+}$ (Ru**2**), have been synthesized and characterized. The binding properties of the two complexes with the RNA poly(U)·poly(A) * poly(U) triplex have been investigated by spectroscopic methods and viscosity measurements. The results presented here indicate that the binding differences of Ru**1** and Ru**2** with the triplex may be attributed to the ancillary ligand effects, suggesting that the

better planarity and greater hydrophobicity of ancillary ligands in Ru**2** are advantageous to the π–π stacking interaction between this Ru(II) complex and the triplex, thus Ru**2** stabilizes the triplex strongly than Ru**1**. In comparison with the third-strand stabilized by those reported Ru(II)-dppz complexes containing dppz units [18b,21], however, the third-strand stabilizing effects of both Ru**1** and Ru**2** are more remarkable, reflecting that the electron-withdraw fluorine substituent on the main ligand dppz of Ru**1** and Ru**2** can probably decrease electrostatic repulsion between the three strands of the triplex, thereby significantly increase the triplex stabilization. Results obtained from this work further confirm that the substituent electron effect of dppz-based ligands and the planarity and hydrophobicity of ancillary ligands play an important role in the triplex stabilizing effects by Ru(II)-dppz complexes. We hope that this work will aid in the understanding of the binding of metal complexes with RNA triplexes, particularly Ru(II) polypyridyl complexes.

Acknowledgements

We would like to thank the National Natural Science Foundation of China (21671165) and Hunan Provincial Natural Science Foundation of China (2016JJ2121) for financial supports.

References

[1] G. Felsenfeld, D.R. Davies, A. Rich, J. Am. Chem. Soc. 79 (1957) 2023–2024.
[2] (a) M. Cooney, G. Czernuszewicz, E.H. Postel, S.J. Flint, M.E. Hogan, Science 241 (1988) 456–459;
(b) A.J. Kinniburgh, A.B. Firulli, R. Kolluri, Gene 149 (1994) 93–100;
(c) V. Buckin, H. Tran, V. Morozov, L.A. Marky, J. Am. Chem. Soc. 118 (1996) 7033–7039;
(d) J.D. Dinman, S. Richter, E.P. Plant, R.C. Taylor, A.B. Hammell, T.M. Rana, Proc. Natl. Acad. Sci. U. S. A. 99 (2002) 5331–5336;
(e) A. Jain, A. Bacolla, P. Chakraborty, F. Grosse, K.M. Vasquez, Biochemistry 49 (2010) 6992–6999.
[3] (a) F.A. Buske, J.S. Mattick, T.L. Bailey, RNA Biol. 8 (2011) 427–439;
(b) A. Bacolla, G. Wang, K.M. Vasquez, PLoS Genet. 11 (2015) e1005696;
(c) G. Devi, Y. Zhou, Z.S. Zhong, D.F.K. Toh, G. Chen, WIREs RNA 6 (2015) 111–128.
[4] (a) G.M. Carbone, S. Napoli, A. Valentini, F. Cavalli, D.K. Watson, C.V. Catapano, Nucleic Acids Res. 32 (2004) 4358–4367;
(b) L.A. Christensen, R.A. Finch, A.J. Booker, K.M. Vasquez, Cancer Res. 66 (2006) 4089–4094;
(c) S. Pandey, A.M. Ogloblina, B.P. Belotserkovskii, N.G. Dolinnaya, M.G. Yakubovskaya, S.M. Mirkin, P.C. Hanawalt, Nucleic Acids Res. 43 (2015) 6994–7004.
[5] S. Das, G.S. Kumar, A. Ray, M. Maiti, J. Biomol. Struct. Dyn. 20 (2003) 703–713.
[6] (a) M. Li, T. Zengeya, E. Rozners, J. Am. Chem. Soc. 132 (2010) 8676–8681;
(b) P. Gupta, O. Muse, E. Rozners, Biochemistry 51 (2012) (63–1461102773).
[7] T. Biver, Coord. Chem. Revie. 257 (2013) 2765–2783.
[8] T.C. Jenkins, C. Med, Chem. 7 (2001) 99–115.
[9] D.P. Arya, R.L. Coffee, J.B. Med, Chem. Lett. 10 (2000) 1897–1899.
[10] D.P. Arya, R.L. Coffee, J.B. Willis, A.I. Abramovitch, J. Am. Chem. Soc. 123 (2001) 4385–4396.
[11] A.K. Shchyolkina, E.N. Timofeev, Y.P. Lysov, V.L. Florentiev, T.M. Jovin, D.J. Arndt-Jovin, Nucleic Acids Res. 29 (2001) 986–995.
[12] M. Polak, N.V. Hud, Nucleic Acids Res. 30 (2002) 983–992.
[13] D.P. Arya, L. Micovic, I. Charles, R.L. Coffee, B. Willis, L. Xue, J. Am. Chem. Soc. 125 (2003) 3733–3744.
[14] (a) D. Bhowmik, G.S. Kumar, Mol. Biol. Rep. 40 (2013) 5439–5450;
(b) D. Bhowmik, S. Das, M. Hossain, L. Haq, G.S. Kumar, PLoS One 7 (2012) e37939.
[15] O. Doluca, A.S. Boutorine, V.V. Filichev, Biochemistry 12 (2011) 2365–2374.
[16] H.J. Lozano, B. García, N. Busto, J.M. Leal, J. Phys. Chem. B 117 (2012) 38–48.
[17] F.J. Hoyuelos, B. García, J.M. Leal, N. Busto, T. Biver, F. Secco, M. Venturini, Phys. Chem. Chem. Phys. 16 (2014) 6012–6018.
[18] (a) J.M. García, V. Leal, R. Paiotta, F. Ruiz, M. Secco, J. Venturini, Phys. Chem. B 112 (2008) 7132–7139;
(b) L.F. Tan, J. Liu, J.L. Shen, X.H. Liu, L.L. Zeng, L.H. Jin, Inorg. Chem. 51 (2012) 4417 − 4419.
[19] (a) M.R. Gill, J.A. Thomas, Chem. Soc. Rev. 41 (2012) 3179 − 3192;
(b) A.C. Komor, J.K. Barton, Chem. Commun. 49 (2013) 3617 − 3630.
[20] (a) R. Sinha, G.S. Kumar, J. Phys. Chem. B 113 (2009) 13410–13420;
(b) E.A. Mesri, E. Cesarman, C. Boshoff, Nat. Rev. Cancer 10 (2010) 707 − 719;
(c) T. Zengeya, P. Gupta, E. Rozners, Angew. Chem. 124 (2012) 12761–12764;
(d) D.P. Arya, Acc. Chem. Res. 44 (2011) 134–146.
[21] (a) W.Z. Tang, Z.Y. Zhu, L.F. Tan, Mol. BioSyst. 12 (2016) 1478–1485;
(b) M.N. Peng, Z.Y. Zhu, L.F. Tan, Inorg. Chem. 56 (2017) 7312 − 7315;
(c) Y.D. Feng, X.H. Liu, S. Ma, F.F. Wang, L.F. Tan, Spectrochim. Acta A 212 (2019) 240–245.
[22] M. Yamada, Y. Tanaka, Y. Yoshimato, S. Kuroda, I. Shimao, Bull. Chem. Soc. Jpn. 65 (1992) 1006–1011.
[23] B.P. Sullivan, D.J. Sullivan, T. Meyer, J. Inorg. Chem. 17 (1978) 3334–3341.
[24] R.B. Nair, C.J. Murphy, J. Inorg. Biochem. 69 (1998) 129–133.
[25] J.R. Lakowicz, G. Webber, Biochemistry 12 (1973) 4161–4170.
[26] X.J. He, L.F. Tan, Inorg. Chem. 53 (2014) 11152–11159.
[27] J.E. Dickeson, L.A. Summers, Aust. J. Chem. 23 (1970) 1023–1027.
[28] J.G. Liu, Q.L. Zhan, L.N. Ji, Transit. Met. Chem. 26 (2001) 733–738.
[29] A.E. Friedman, J.C. Chambron, J.P. Sauvage, N.J. Turro, J.K. Barton, J. Am. Chem. Soc. 112 (1990) 1146–4960.
[30] E.J.C. Olson, D. Hu, A. Hormann, A.M. Jonkman, M.R. Arkin, E.D.A. Stemp, J.K. Barton, P.F. Barbara, J. Am. Chem. Soc. 119 (1997) 11458–11467.
[31] S.D. Choi, M.S. Kim, S.K. Kim, P. Lincoln, E. Tuite, B. Nordén, Biochemistry 36 (1997) 214–223.
[32] A. Kabir, G.S. Kumar, Mol. BioSyst. 10 (2014) 1172–1183.
[33] J.S. Paige, K.Y. Wu, S.R. Jaffrey, Science 333 (2011) 642–646.
[34] (a) C.V. Kumar, J.K. Barton, N.J. Turro, J. Am. Chem. Soc. 107 (1985) 5518–5523;
(b) S. Satyanarayana, J.C. Dabrowiak, J.B. Chaires, Biochemistry 31 (1992) 9319–9324.
[35] Z.Y. Zhu, M.N. Peng, J.W. Zhang, L.F. Tan, J. Inorg. Chem. 169 (2017) 44–49.
[36] H. Zhang, X.W. Liu, X.J. He, Y. L, L.F. Tan, Metallomics 6 (2014) 2148–2156.
[37] S. Maa, F.F. Wanga, Y.D. Feng, X.H. Liu, L.F. Tan, Polyhedron 162 (2019) 277–284.
[38] S. Das, G.S. Kumar, A. Ray, M.J. Maiti, Biomol. Struct. Dyn. 20 (2003) 703–714.
[39] B. Tijana, N. Olga, H. Anna, Z. Lenka, V. Oldrich, K. Jana, H. Abraha, P. Simon, J.S. Peter, B. Viktor, B.J. Med. Chem. 51 (2008) 5310–5319.
[40] M.N. Patel, M.R. Chhasatia, D.S. Gandhi, Bioorg. Med. Chem. 17 (2009) 5648–5655.
[41] H.J. Xi, E. Davis, N. Ranjan, L. Xue, D. Hyde-Volpe, D.P. Arya, Biochemistry 50 (2011) 9088–9113.